

Electron and stochastic beam cooling for intensive heavy ion beams at NICA complex: Experiments and plans

E. Syresin¹ Y. Tamashevich^{1†} V. Lebedev¹ A. Butenko¹ I. Gorelyshev¹ I. Meshkov¹ K. Osipov¹
 Yu. Prokofichev¹ V. Shpakov¹ S. Semenov¹ A. Sergeev¹ A. Sidorin¹ R. Timonin¹ G. Trubnikov¹
 M. Bryzgunov² A. Bubley² V. Panasyuk² V. Parkhomchuk² V. Reva²

¹Joint Institute for Nuclear Research, Dubna, Russia

²Budker Institute of Nuclear Physics, Novosibirsk, Russia

Abstract: The Nuclotron-based Ion Collider fAcility (NICA), currently under construction at JINR, is expected to conduct its first beam tests in the second half of 2025. The NICA project is designed to provide colliding beams for investigating heavy stripped ion collisions at energies of 4.5 GeV/u. The NICA accelerator complex comprises several components: the operational heavy ion linac HILAC with an energy of 3.2 MeV/u, superconducting Booster synchrotron with a maximum energy of 600 MeV/u, superconducting Nuclotron synchrotron capable of accelerating gold ions to 3.9 GeV/u, and two storage rings with two interaction points currently under installation. The system includes two electron cooling units—one in the Booster synchrotron with a maximum electron energy of 60 keV, and another in the Collider with two electron beams, each with a maximum energy of 2.5 MeV. Additionally, two stochastic cooling systems are integrated into the setup. The status of the NICA accelerator complex, including its cooling systems, is presented. Experimental results from electron cooling studies conducted during the commissioning of the injection complex are reported. Plans for the further development and application of the electron and stochastic cooling systems are also described.

Keywords: NICA, electron beam cooling, stochastic beam cooling, heavy ion beams, ion collider

DOI: 10.1088/1674-1137/adb4d0 **CSTR:** 32044.14.ChinesePhysicsC.49074003

1. NICA INJECTION COMPLEX

The Nuclotron-based Ion Collider fAcility (NICA) is currently being commissioned at JINR [1, 2]. The NICA complex comprises two collider rings designed for head-on collisions at two interaction points and an injection system [3, 4], which includes a linac and two synchrotrons (Booster and Nuclotron).

The Krion-6T ion source [5] generates beams of highly multicharged ions. For Collider operations, using $^{209}\text{Bi}^{35+}$ and $^{197}\text{Au}^{79+}$ ions is planned, while $^{124}\text{Xe}^{28+}$ ions were used during Run IV (September 2022 – February 2023). These ions are also expected to be used during the initial stages of Collider commissioning. In Run IV, approximately 25% of the ions extracted from the source had the desired charge state, with a typical intensity of approximately 10^8 ions per pulse for the targeted charge. After electrostatic acceleration to 17 keV/u, the beam is further accelerated in the RFQ and two sections of the DTL heavy ion linac (HILAC) [6] to an energy of 3.2 MeV/u. The beam is then injected into the Booster using single-turn injection.

The Booster is a superconducting synchrotron designed to accelerate heavy ions to an energy of 600 MeV/u ($A/Z \approx 6$). According to the Collider design report [3], the required beam intensity is approximately 10^9 ions per pulse from the injection complex, with a cycle duration of 4–5 s.

The xenon ion beam extracted from the Krion-6T ion source exhibited 5–6 different charge states, with the targeted charge state ($Z = 28$) constituting approximately 25% of the beam. At the HILAC exit, the intensity of the $^{124}\text{Xe}^{28+}$ ions is approximately 5×10^7 ions, with a total beam pulse duration of 12–15 μs . However, this intensity remains about an order of magnitude lower than the level required for the Collider [3].

To address this, an initial strategy involved accumulating the beam in the transverse plane of the Booster using multiple injections combined with beam damping with electron cooling [7]. Given that the longitudinal cooling rate is thrice faster than that of transverse cooling, the current plan emphasizes accumulation in the longitudinal plane [8]. Transverse cooling is further suppressed for high-amplitude particles because the electron

Received 22 January 2025; Accepted 19 February 2025; Published online 20 February 2025

[†] E-mail: tamashevich@jinr.ru

©2025 Chinese Physical Society and the Institute of High Energy Physics of the Chinese Academy of Sciences and the Institute of Modern Physics of the Chinese Academy of Sciences and IOP Publishing Ltd. All rights, including for text and data mining, AI training, and similar technologies, are reserved.

beam radius is approximately half the beam size at the acceptance boundary. To achieve a tenfold accumulation (Fig. 1(a)), the Booster cools the stored bunch during the accumulation process, thereby reducing its length to less than half of the ring circumference, while the remaining half is allocated for beam injection.

The beam pulse duration from the ion source was reduced to 4 μs (Fig. 1(b)).

II. BOOSTER ELECTRON COOLING

The Booster electron cooling system [9–11], designed and manufactured by BINP SB RAS, features a maximum electron energy of 50 keV and cooling length of 2.5 m [3] (see Table 1 and Fig. 2).

During Collider operations, the aforementioned system will be employed at the injection energy of 3.2 MeV/u for beam accumulation and cooling. Although the Booster electron cooling system was tested using different ion species, it was not regularly used for beam delivery to users until the final stages of Run IV.

Booster electron cooling was investigated during the 2nd [4] and 4th [12] Runs. Measurements were conducted at the injection energy of 3.2 MeV/u using $^{56}\text{Fe}^{14+}$ [4] (Figs. 3 and 4) and $^{124}\text{Xe}^{28+}$ ions. In the 4th Run, the acceleration of the $^{124}\text{Xe}^{28+}$ ions began 230 ms after injection. Although this interval was short, it effectively cooled the ions, thereby resulting in a threefold bunch length reduction with an electron beam current of 50 mA

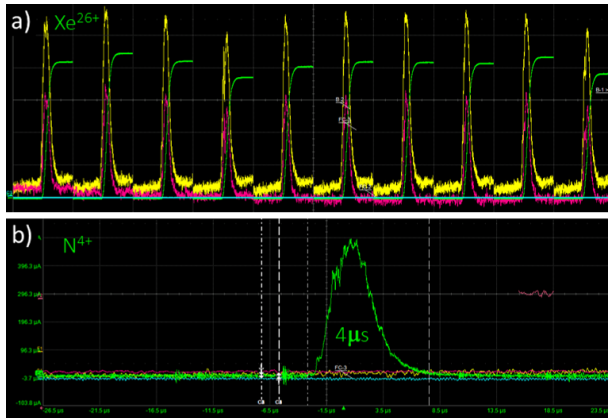


Fig. 1. (color online) (a) Multi-cycle injection with ten pulses from HILAC; (b) dependence of nitrogen ion beam current intensity on time.

Table 1. Parameters of the Booster electron cooling system.

Maximal electron energy	50 keV
Electron beam current	0–1 A
Length of the cooling section	2.5 m
Electron beam radius	14 mm

(Fig. 5).

Figure 6 compares the time evolution of bunch duration with electron cooling off (red circles) and on (blue stars). These experimental data indicate a longitudinal cooling time of approximately 70 ms.

Transverse cooling effects were observed using a beam viewer installed in the Booster-Nuclotron transfer line, thereby enabling the imaging of the transverse intensity distribution post-acceleration. As shown in Figs. 7 and 8, cooling reduced the full width at half maximum (FWHM) beam transverse sizes from 7.81 to 3.34 mm horizontally and from 5.38 to 1.63 mm vertically.

The reduction in beam emittances led to decreased beam losses during acceleration, which in turn doubled the intensity of the beam extracted from the Nuclotron for the fixed-target BM@N experiment. Consequently, the



Fig. 2. (color online) Image of the Booster electron cooling system with the 2.5 m cooling section designed for a maximum electron energy of 50 keV.

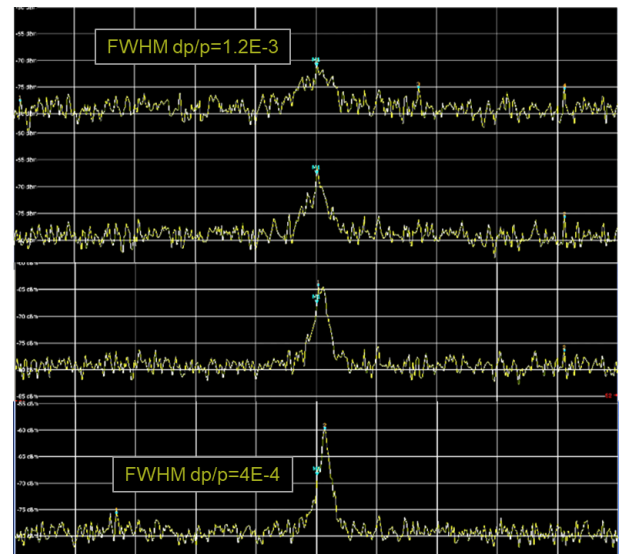


Fig. 3. (color online) Evolution of the Schottky noise signal at the 4th harmonic of the revolution frequency for $^{56}\text{Fe}^{14+}$ ions at 3.2 MeV/u. The top trace shows the signal without cooling, while the bottom trace illustrates the signal after cooling.

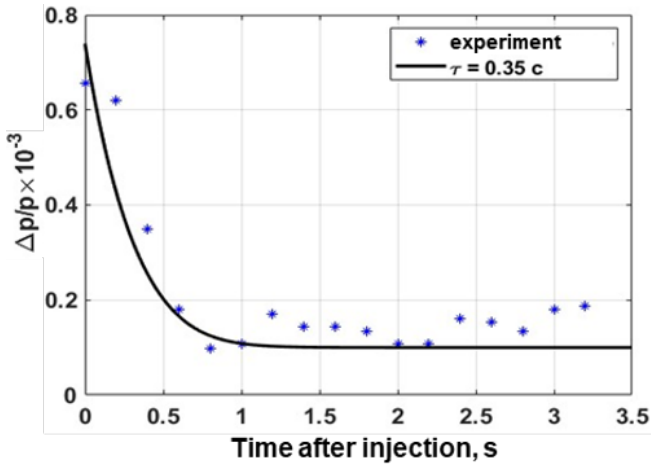


Fig. 4. (color online) Dependence of the momentum spread of the $^{56}\text{Fe}^{14+}$ ion beam on time at an ion energy of 3.2 MeV/u and an electron beam current of 76 mA. Measurements were performed using a continuous beam with Schottky noise.

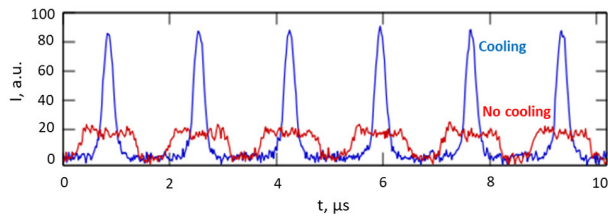


Fig. 5. (color online) Longitudinal bunch profiles of $^{124}\text{Xe}^{28+}$ ion beams without (red line) and with (blue line) electron cooling at an electron beam current of 50 mA. Measurements were obtained using a fast beam current monitor shortly before beam acceleration, with RF voltage applied.

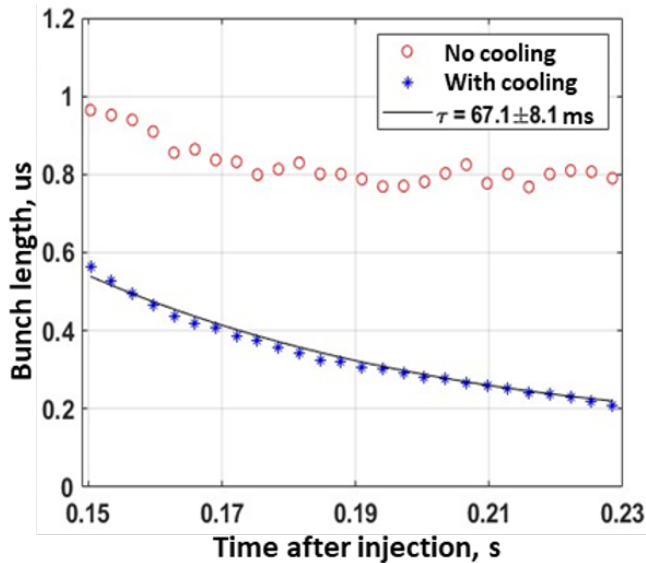


Fig. 6. (color online) Dependence of bunch duration on time with electron cooling enabled (blue stars) and disabled (red circles) for $^{124}\text{Xe}^{28+}$ ions, measured during Run IV.

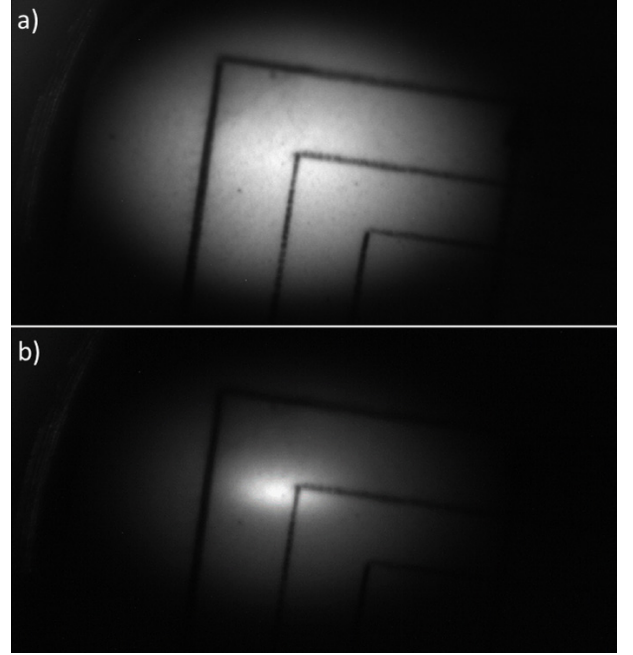


Fig. 7. (color online) Transverse profiles of the ion beam captured on the beam viewer (luminophore screen) without electron cooling (a) and with electron cooling (b). The beam intensity was reduced to prevent saturation of the screen.

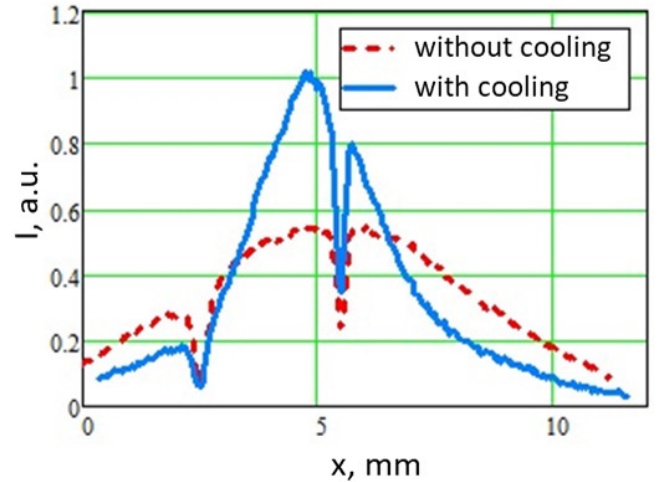


Fig. 8. (color online) Transverse beam profiles in the transfer channel without Booster electron cooling (red dotted line) and with electron cooling (blue solid line).

number of $^{124}\text{Xe}^{54+}$ nuclei reached 10^7 per pulse (Fig. 9).

III. BEAM ACCUMULATION IN BOOSTER

To achieve Collider operations at designed parameters, the number of ions delivered from the injection chain to the Nuclotron at its maximum energy must be increased by a factor of about 30 compared to recent runs. This is owing to a 20-fold shortfall in the ion source intensity compared to the design specification. The short-

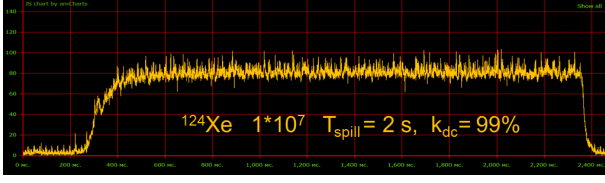


Fig. 9. (color online) Dependence of beam intensity on time for the $^{124}\text{Xe}^{54+}$ ion beam extracted from the Nuclotron. The extraction efficiency is approximately 30%, while the coefficient k_{dc} indicates the time uniformity of the extracted beam intensity.

fall will be addressed by ion accumulation in the Booster, facilitated by electron cooling, and by minimizing beam losses during acceleration and transfer.

Since longitudinal cooling is significantly faster than transverse cooling, accumulation will be performed in the longitudinal plane. Electron cooling will create space for subsequent injections. Calculations, supported by experimental results, indicate an optimal stacking rate of ≈ 10 Hz. Between 10 and 15 injections will be needed to reach the space charge limit at the injection energy. Consequently, around 1 s of the 5-s acceleration cycle will be dedicated to beam accumulation in the Booster.

A 10 Hz operation of the Krion-6T ion source with 10 pulses was recently demonstrated for $^{124}\text{Xe}^{28+}$ ions (Fig. 1(a)). Optimizing the ion source tuning increased the total extracted charge from 2.4 to 3 nC. Further improvements included shortening the ion pulse duration from ≈ 15 μs to 4 μs (Fig. 1(b)) by reshaping the holding electrodes to produce a uniform electric field and implementing a specially programmed electrode power supply.

The low-energy beam transport, coupled with the linac and transfer line quadrupole power supplies, has been configured to support 10 consecutive injection pulses at a 10-Hz repetition rate from the linac. Beam accumulation in the Booster will occur at the first RF harmonic, with a bucket height of $(\Delta p/p)_{\text{max}} = 1.8 \times 10^{-3}$, which maximizes the cooling rate. Achieving this requires an RF voltage of 200 V.

Half of the Booster ring will be used for injection, and the other half for accumulation is showed in Fig. 10. A new injection will occur only after the previous bunch is cooled to the core. The continuous presence of the first RF harmonic will minimal affect particles with high synchrotron amplitudes. The total number of accumulated ions and depth of cooling will be limited by the ion bunch space charge. Approximately 10^9 ions of $^{209}\text{Bi}^{35+}$ can be stored.

To minimize longitudinal emittance growth, rebunching during Booster acceleration will be avoided. Instead, the entire acceleration process will occur at the first harmonic. Since the RF frequency at the start of the cycle is outside the nominal operational range, the initial RF voltage will be reduced to approximately 1.5 kV. As the

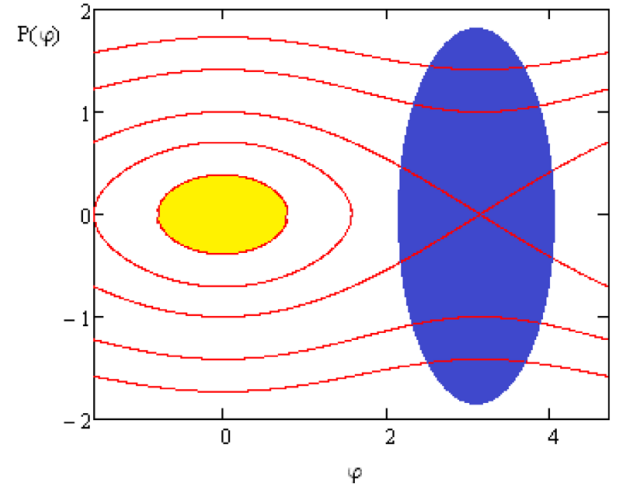


Fig. 10. (color online) Schematic of Booster ion accumulation in longitudinal phase plane facilitated by electron cooling.

beam accelerates, the RF voltage gradually increases, reaching its nominal value of 10 kV at a beam energy of around 100 MeV/u. This approach will extend the acceleration cycle by 300 ms, which would otherwise be required for rebunching.

IV. COLLIDER

The NICA Collider [1–3, 13] comprises two storage rings (Fig. 11) with two interaction points (IPs). The main operational parameters for fully stripped $^{209}\text{Bi}^{83+}$ ions are presented in Table 2.

The electron cooling system [14] for the Collider will be operating at a maximum electron energy of 2.5 MeV. The key parameters of the system are presented in Table 3. It is designed for ion accumulation and bunch formation at kinetic energies ranging from 1.0 to 4.5 GeV/u. The system includes a 6 m solenoid cooling section with a magnetic field of 0.1 T and a maximum electron beam current of 1 A (Fig. 12). The cooling system construction began at BINP in 2016, with assembly work scheduled for 2025 and electron beam operation set to start in 2026.

The RF barrier bucket technique [3] facilitates efficient particle accumulation, enabling the achievement of high intensities. The Collider receives one bunch from the Nuclotron every 4 s, containing $(0.2\text{--}2) \times 10^9$ nuclei. Figure 13 illustrates the results of modeling calculations showing the dependence of the stored number of $^{209}\text{Bi}^{83+}$ ions in the Collider ring at an ion energy of 3 GeV/u. The cooling time for these ions is expected to be approximately 100 s at energies of 3–4.5 GeV/u.

At a cooling time of 300 s, the longitudinal acceptance of the RF1 barrier is fully utilized after 25 ion injection cycles. The decrease in the stored intensity for injection cycles exceeding $n > 25$ (Fig. 13) is attributed to ion losses caused by an increase in momentum owing to int-



Fig. 11. (color online) Assembly process of the Collider rings at the NICA facility.

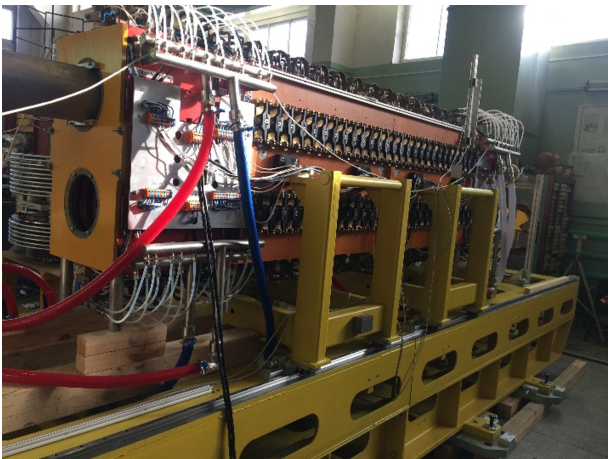


Fig. 12. (color online) Solenoidal section of the Collider electron cooling system.

Table 2. Key parameters of the NICA Collider.

Circumference	503.04 m
Maximum magnetic rigidity	45 T m
Average residual gas pressure	$<1 \times 10^{-8}$ Pa
Maximum dipole magnets field	1.8 T
Kinetic energy of gold nuclei	1–4.5 GeV/u
Luminosity at maximum energy	$1 \times 10^{27} \text{ cm}^{-2} \text{ s}^{-1}$

Table 3. Key parameters of the Collider electron cooling system.

Electron energy	0.2–2.5 MeV
Energy stability, $\Delta E/E$	$<1 \times 10^{-4}$
Electron beam current	0.1–1 A
Cooling section length	6 m
Solenoid magnetic field	0.05–0.2 T
Field homogeneity, $\Delta B/B$	$<1 \times 10^{-5}$

rabeam scattering.

Precooling in the Booster reduces the relative rms momentum ($\Delta p/p$) by a factor of 3, down to 4×10^{-4} , thereby allowing ions to be stored for up to 75 injection cycles. Under these conditions, a cooling time (τ_{cool}) of 300 s allows for stack storage with the required intensity.

The Collider electron cooling system is crucial in achieving an ion momentum spread of $\Delta p/p \approx 10^{-3}$ and a bunch length of 0.6 m (Fig. 14).

Achieving the design luminosity of $1 \times 10^{27} \text{ cm}^{-2} \text{ s}^{-1}$ will require the full-scale commissioning of the RF3 system, electron cooling, and full energy extraction from the Nuclotron, expected by 2026.

In addition to electron cooling [14], the Collider will feature a stochastic cooling system (SCS) capable of

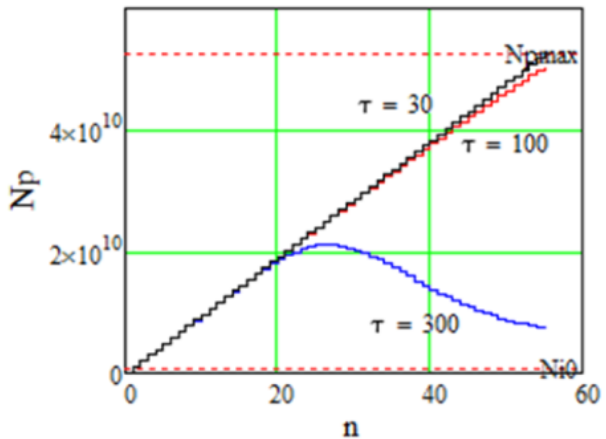


Fig. 13. (color online) Relationship between the number of stored ions (N_p) and injection cycles (n) for different cooling time constants (τ).

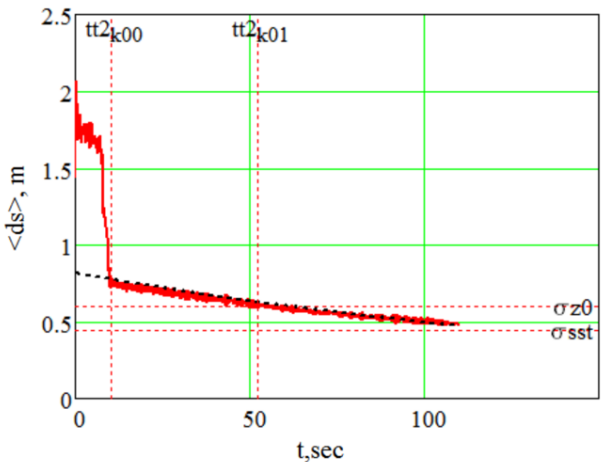


Fig. 14. (color online) Dependence of bunch length on time during RF3 bunching and electron cooling, with a cooling duration of 100 s.

Table 4. Key parameters of the Collider stochastic cooling system.

Ion energy for $^{209}\text{Bi}^{83+}$	2.5–4.5 GeV/u
Momentum cooling method	Filter
Full bandwidth	640–3240 MHz
Channel 1	640–960 MHz
Channel 2	960–1440 MHz
Channel 3	1440–2160 MHz
Channel 4	2160–3240 MHz
Cable distance Pickup-Kicker	≈ 120 m
Beam distance Pickup-Kicker	186 m () 194 m (\perp)
Pickup shunt impedance	200 Ω () 4 Ω/mm (\perp)
Kicker shunt impedance	800 Ω () 16 Ω/mm (\perp)
Pickup temperature	300 K

cooling all three degrees of freedom [3, 15]. The key parameters of the system are presented in Table 4. The SCS operates at ion energies ranging from 2.5–4.5 GeV/u with a frequency range of 640–3200 MHz, which is capable of cooling bunches containing 3.1×10^9 $^{209}\text{Bi}^{83+}$ ions.

The SCS employs pickup electrodes, kickers, signal delay system blocks, cascaded solid-state amplifiers and preamplifiers, and a comb filter system. A distinctive feature of the NICA SCS is the installation of pickups and kickers around ceramic vacuum chambers. Each cooling system is divided into four bands as presented in Table 4.

The SCS hardware will be installed in two stages. The first stage, covering $\approx 25\%$ of the system and operating at frequencies of 960–1440 MHz, will be completed by the end of 2024 for longitudinal cooling. The final stage, incorporating the full system, will be implemented in 2026.

References

- [1] G. Trubnikov *et al.*, *Project of the Nuclotronbased ion collider facility (NICA) at JINR*, Proceedings of EPAC08 (Genoa, Italy, 2008)
- [2] V. D. Kekelidze *et al.*, *Three stages of the NICA accelerator complex*, Journal of Physics: Conference Series (IOP Publishing, 2016), Vol. 668, 1., p. 012023
- [3] Ed. I. Meshkov and G. Trubnikov, *Technical Project of NICA Acceleration Complex*, 2015
- [4] A. V. Butenko *et al.*, *NICA Booster: a new generation superconducting synchrotron*, Uspekhi Fizicheskikh Nauk, 193.2, p. 206, 2023
- [5] E. D. Donets *et al.*, *ESIS ions injection, holding and extraction control system*, EPJ Web of Conferences (EDP Sciences, 2018), Vol. 177, p. 08002
- [6] A. V. Butenko *et al.*, *The heavy ion injector at the NICA project*, Proc. LINAC'14, p. 1068, 2014
- [7] E. M. Syresin, *Phys. Part. Nuclei Lett.* **12**, 591 (2023)
- [8] A. V. Butenko *et al.*, *Phys. Part. Nuclei Lett.* **21**, 212 (2023)
- [9] M. Bryzgunov *et al.*, *Status of the electron cooler for NICA booster and results of its commissioning*, Proceedings of the 12th Workshop on Beam Cooling and Related Topics COOL-2019 (Novosibirsk, Russia, 2019), p. 22
- [10] L. V. Zinovyev *et al.*, *Phys. Part. Nuclei Lett.* **15**, 745 (2018)
- [11] E. Syresin *et al.*, *NICA synchrotrons and their cooling systems*, Proceedings of the 13th International Workshop on Beam Cooling and Related Topics (COOL21) (Novosibirsk, Russia, 2021), p. 1
- [12] O. I. Brovko *et al.*, *NICA ion collider and its acceleration complex*, Proceedings of 14th International Particle Accelerator Conference IPAC'23 (Venice, Italy, 2023), p. 616
- [13] E. Syresin *et al.*, *NICA ion collider and plans of its first operations*, Proceedings of the 13th International Particle Accelerator Conference (IPAC'22, Bangkok, Thailand, 2022), p. 1819
- [14] M. I. Bryzgunov *et al.*, *Phys. Part. Nuclei Lett.* **17**, 425 (2020)
- [15] K. G. Osipov, *Design and Optimization of the NICA Longitudinal Stochastic Cooling Pickup/Kicker*, XXVII Russian Particle Accelerator Conference (RuPAC-2021, Alushta, Russia, 2021, TUPSB02)